HHS Public Access

Author manuscript

J Neurosci Res. Author manuscript; available in PMC 2019 March 01.

Novel luciferase – opsin combinations for improved luminopsins

Sung Young Park[1], **Sang-Ho Song**[2,3], **Brandon Palmateer**[4,5], **Akash Pal**[4,5], **Eric D. Petersen**[4,5], **Gabrielle P. Shall**[4], **Ryan M. Welchko**[4], **Keiji Ibata**[6,7], **Atsushi Miyawaki**[6], **George J. Augustine**[1,2,3], and **Ute Hochgeschwender**[4,5]

[1]Center for Functional Connectomics, Korea Institute of Science and Technology, Seoul 136-701, Republic of Korea

[2]Lee Kong Chian School of Medicine, Nanyang Technological University, Singapore 138673, Singapore

[3]Institute of Molecular and Cell Biology, Singapore 138673, Singapore

[4]Neuroscience Program, Central Michigan University, Mt. Pleasant, MI, 48859, USA

[5]College of Medicine, Central Michigan University, Mt. Pleasant, MI, 48859, USA

[6]Laboratory for Cell Function Dynamics, Brain Science Institute, Riken, Saitama, 351-0198, Japan

[7]School of Medicine, Keio University, Tokyo, 160-8582, Japan

Abstract

Previous work has demonstrated that fusion of a luciferase to an opsin, to create a luminescent opsin or luminopsin, provides a genetically-encoded means of manipulating neuronal activity via both chemogenetic and optogenetic approaches. Here we have expanded and refined the versatility of luminopsin tools by fusing an alternative luciferase variant with high light emission, *Gaussia* luciferase mutant GLucM23, to depolarizing and hyperpolarizing channelrhodopsins with increased light sensitivity. The combination of GLucM23 with *Volvox* channelrhodopsin-1 produced LMO4, while combining GLucM23 with the anion channelrhodopsin, iChloC, yielded iLMO4. We found efficient activation of these channelrhodopsins in the presence of the luciferase substrate, as indicated by responses measured in both single neurons and in neuronal populations of mice and rats, as well as by changes in male rat behavior during amphetamine-induced rotations. We conclude that these new LMOs will be useful for bimodal opto- and chemogenetic analyses of brain function.

Graphical Abstract

Corresponding author: Ute Hochgeschwender, M.D., Neuroscience Program and College of Medicine, Central Michigan University, 1280 SE Campus Drive, CMED 2405, Mount Pleasant, MI 48859, Phone: 989-774-1471, Fax: 989-774-1215, hochg1u@cmich.edu.

CONFLICT OF INTEREST STATEMENT

All authors declare that they have no competing financial interests.

ROLES OF AUTHORS

All authors had full access to all the data in the study and take responsibility for the integrity of the data and the accuracy of the data analysis. Study concept and design: GJA, UH. Acquisition of data: SYP, S-HS, BP, AP, EDP, UH. Analysis and interpretation of data: SYP, S-HS, BP, AP, EDP, AM, GJA, UH. Drafting of the manuscript: SYP, SHS, GJA, UH. Statistical analysis: SYP, S-HS, AP, EDP, UH. Obtained funding: GJA, UH. Technical and material support: GPS, RMW, KI, AM. Study supervision: GJA, UH.

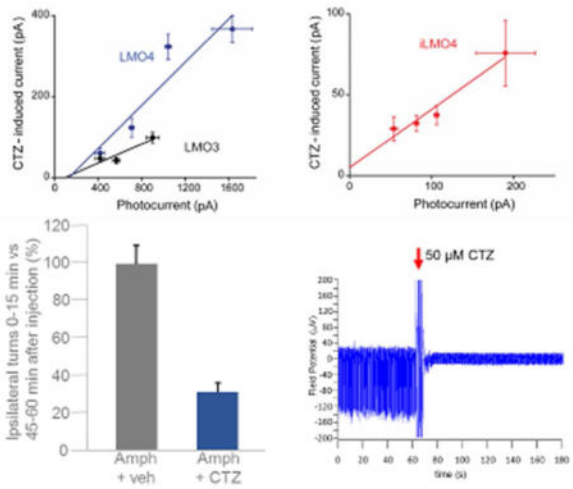

Fusing a luciferase variant with high light emission, GLucM23, to depolarizing and hyperpolarizing channelrhodopsins significantly increased efficiency of coupling between the luciferase light source and the opsin actuator. The resulting improved bioluminescence-driven optogenetic activation and silencing was demonstrated in single cell recordings, multi-electrode recordings, and by affecting behavior.

Keywords

bioluminescence; optogenetics; chemogenetics; GLucM23; iChloC; 6-OHDA rat

INTRODUCTION

Interrogation of neural circuits at a wide range of spatial and temporal scales is necessary to elucidate the relationship between neural activity and behavior. For this purpose, both optogenetic (Fenno et al., 2011) and chemogenetic (Sternson and Roth, 2014) probes have proven very valuable, because of their ability to manipulate the electrical activity of genetically-defined populations of neurons. Previous work has developed a toolset that integrates opto- and chemogenetic approaches by fusing a light-emitting luciferase to an optogenetic light-responsive element, resulting in a luminescent opsin, or luminopsin (LMO; Berglund et al., 2013; Tung et al., 2015; Berglund et al., 2016). In these luminopsins, bioluminescence produced by oxidation of a diffusible luciferin substrate by the luciferase enzyme activates a tethered, nearby opsin. Depending on the biophysical properties of the opsin, the light generated by the luciferase can either excite or inhibit target neurons expressing the LMO. Such integration of opto- and chemogenetic approaches allows manipulation of neural activity over a range of spatial and temporal scales in the same experimental animal. Specifically, LMOs allow rapid optogenetic control of the activity of subsets of neurons as well as slower chemogenetic control of the activity of entire populations of neurons.

Initially, wild type *Gaussia* luciferase (GLuc; Verhaegen and Christopoulos, 2002) was combined with channelrhodopsin 2 (ChR2; Nagel et al., 2003) to yield the excitatory LMO1

(Berglund et al., 2013), while combination of the red-shifted *Renilla* luciferase version TagRFP-RLuc (Dragulescu et al., 2011) with *Natronomonas* halorhodopsin (NpHR; Gradinaru et al., 2008) resulted in the inhibitory iLMO1 (Tung et al. 2015). The performance of subsequent LMO versions was significantly improved by using luciferase variants with higher light emission, such as the GLuc variants 'slow burn' (sbGLuc; Welsh et al., 2009) and 'superluminescent' (slGLuc; Kim et al., 2011), as well as the RLuc-based luciferase–fluorescent fusion protein Nano-lantern (Saito et al., 2012). These probes allowed activation and silencing of neurons via non-invasive peripheral application of the luciferase substrate in freely moving mice and rats, resulting in observable changes in their behavior (Berglund et al., 2016; Tung et al., 2015).

While the current LMOs are usable, their performance is not fully optimized. Here we have explored the potential of a new *Gaussia* luciferase mutant with very efficient light generation, GLucM23 (Lindberg et al., 2013), as the light-emitting moiety in LMOs. By fusing GLucM23 to the depolarizing opsin VChR1 we created a fourth-generation excitatory LMO, LMO4. Similarly, by fusing GLucM23 to a hyperpolarizing anion channelrhodopsin, iChloC (Wietek et al., 2015), we created a novel inhibitory luminopsin, iLMO4. Validation of these new constructs, both *in vitro* and *in vivo*, revealed that these new luminopsins have the highest known coupling between the luciferase enzyme and the opsin actuators. We conclude that these new LMOs are useful additions to the luminopsin toolset for bimodal opto- and chemogenetic experiments.

MATERIALS AND METHODS

Constructs

The generation of LMO plasmids is described in detail in Berglund et al. (2013). For the new versions of LMOs, the wild type *Gaussia* luciferase sequence in LMO2 (GLuc-VCHR1-EYFP) was replaced by the mutated version GLucM23 to generate LMO4 (GLucM23-VChR1-EYFP). Switching out VChR1 with the synthesized sequence for iChloC (Genscript, Piscataway, NJ) generated iLMO4 (GLucM23-iChloC-EYFP). For viral vectors the coding sequences of LMO4 and iLMO4 were cloned into an AAV vector downstream of a human synapsin promoter as described previously (Berglund et al., 2016).

Cell Culture

Human embryonic kidney fibroblasts (HEK293, RRID:CVCL_0045, and HEK293FT, RRID:CVCL_6911) were grown in Dulbecco's modified Eagle's medium (DMEM) supplemented with 10% fetal bovine serum, 100 U penicillin and 0.1 mg streptomycin per milliliter, at 37°C and 5% CO_2 in a humidified atmosphere. Cells were transfected using Lipofectamine 2000 (Invitrogen, Waltham, MA) according to the manufacturer's protocol. For luminescence experiments 1×10^4 cells were seeded in white 96 well plates (BD Falcon, Franklin Lakes, NJ). Cells were used for luminescence experiments 36 hours after transfection.

For *in vitro* electrophysiology studies, primary hippocampal neurons were cultured from newborn mouse pups (P0 to P2) of both sexes of strain B6129F1 hybrid

(RRID:IMSR_TAC:b6129) as described previously (Berglund et al., 2013). Lipofection was used for transfecting cultured neurons on days *in vitro* (DIV) 2 to 4. We used 1/10th of the recommended amount of Lipofectamine and otherwise followed the manufacturer's protocol. Cells were plated in culture medium consisting of Neurobasal Medium (Invitrogen) containing B-27 (Invitrogen), 2 mM Glutamax (Invitrogen), and 5% FCS (NB-FCS). The medium was replaced with culture medium without serum the next day (NB-Plain).

For multi-electrode array experiments, primary neurons were collected from embryonic day 18 rat embryos of both sexes from Sprague Dawley females (RRID:RGD_5508397) obtained directly from a commercial vendor (Harlan) or from BrainBits, LLC. Neurons were transduced with virus on DIV2. Virus was added to the culture medium (1 μl per well of concentrated stocks). All supplements were purchased from Gibco/Invitrogen/Thermo Fisher unless indicated otherwise.

Virus

AAVs carrying LMOs were produced by transfecting subconfluent HEK293FT cells per 10 cm culture dish with 24 μg of the helper plasmid pAd delta F6, 20 μg of the serotype plasmid AAV2/9, and 12 μg of the LMO3 plasmid using Lipofectamine 2000. After 72 h, supernatant was harvested from culture plates and virus was purified from cells and supernatant following the method of Guo et al. (2012), but without the partitioning step in the aqueous two-phase system (Berglund et al., 2016). Viral titers were determined by q-PCR for the WPRE element. Preparations with titers ranging from 1×10^{10} to 1×10^{13} vg/ml were used in this study.

Coelenterazine

The luciferin, coelenterazine (CTZ), was purchased from Nanolight Technology (Pinetop, AZ). For *in vitro* experiments coelenterazine free base, the natural form of CTZ (Nanolight cat. no. 303), was dissolved in NanoFuel (Nanolight cat. no. 399) or acidified ethanol (0.06 N HCl). Reconstituted CTZ was pre-diluted 1:500 in NB-Plain and added to neuron cultures for a final concentration of 100 μM for recordings. For *in vivo* experiments, water soluble CTZ (Nanolight cat. no. 3031) was used, and water-soluble buffer only, without CTZ (Nanolight cat. no. 3031C), was used as a vehicle control.

Bioluminescence Imaging of Cells

For measuring luminescence from HEK cells, reconstituted and diluted CTZ was added to the culture medium immediately before imaging to the final concentration indicated in the experiment. Luminescence was measured using an IVIS Lumina LT In Vivo Imaging System (PerkinElmer, Waltham, MA) with Living Image 4.5.2 software (RRID:SCR_014247). Images were displayed as a pseudo-color photon counted image. Regions of interest were defined using an automatic intensity contour procedure to identify bioluminescent signals with intensities significantly greater than background. The sum of the photon counts in these regions was then calculated.

Electrophysiology and Bioluminescence Imaging in Neurons

Whole-cell patch clamp recordings were made from cultured hippocampal neurons, as described in Berglund et al. (2013, 2016), using an EPC-9D amplifier (HEKA Elektronik, Lambrecht, Germany). For voltage-clamp measurements of photocurrents, neurons were held at a holding potential of −60 mV. When measuring light-induced potential changes, neurons were held at the zero current level in current-clamp mode. Recording pipettes had resistances of 4–5 MΩ and were filled with an internal solution containing 140 mM K-gluconate, 2 mM $MgCl_2$, 0.5 mM $CaCl_2$, 10 mM HEPES, 4 mM Na2-ATP, 0.4 mM Na3-GTP, and 5 mM EGTA (pH 7.1 titrated with KOH). The extracellular solution consisted of 150 mM NaCl, 3 mM KCl, 2 mM $CaCl_2$, 2 mM $MgCl_2$, 20 mM D-glucose, and 10 mM HEPES (pH 7.35, titrated with NaOH).

Photocurrents were measured while illuminating neurons with a mercury lamp via a GFP filter cube (excitation, 465–495 nm); these currents provided a measure of the total surface expression of LMO4 or iLMO4 in each cell. Reconstituted CTZ (100 μM) in extracellular solution was bath-applied to a recording chamber for recording CTZ-induced responses, either photocurrents under voltage clamp or potential changes under current clamp.

Bioluminescence was imaged simultaneously on the same microscope (Olympus IX70), without a filter cube, by using a cooled CCD camera, CoolSNAP fx (Photometrics, Tucson, AZ,) with 4-by-4 binning and 5 s exposure. Metamorph (Molecular Devices, Sunnyvale, CA; RRID:SCR_002368) and ImageJ software (NIH, Bethesda, MD; RRID:SCR_003070) were used for image acquisition and analysis. Experiments were performed at room temperature (21–24 °C). For synchronization of recording and imaging, an output signal from the camera was also used to trigger electrophysiological recording.

Multi Electrode Arrays

For multi electrode array (MEA) experiments, 1-well MEA plates (60MEA200/30iR-Ti; MultiChannel Systems, Tübingen, Germany) were used. MEA plates were sterilized by autoclaving and treated with FBS before coating with 0.1% polyethyleneimine and 10 μg/ml laminin. Neurons were plated on top of the electrodes in a drop containing 4×10^4 cells in 10 μl of Neurobasal media with FBS (see above). Once the cells adhered to the surface, the wells were slowly flooded with media and plates were returned to the incubator. The following day (DIV2) the medium was replaced with culture medium without serum containing adeno associated virus. The medium was replaced every 3 to 4 days thereafter. All-*trans* retinal (R2500; Sigma-Aldrich, St. Louis, MO) was added to the culture medium to 1 μM final concentration before electrophysiological recordings. Consistently spiking neurons were used for recordings on DIV 10 to 19. A micropipette was used to add CTZ in a drop at 1:50 dilution of the MEA volume for a final concentration of 100 μM. Recordings were carried out with a MEA 2100 Lite head stage and amplifier with a sample rate of 10,000 Hz. All MEA analysis was done offline with MC Rack software (MultiChannel Systems; RRID:SCR_014955) and NeuroExplorer (RRID:SCR_001818). Spikes were counted when the extracellular recorded signal exceeded 5 standard deviations of the baseline noise.

Animals

Experimental procedures on cultured mouse neurons were approved by the Institutional Animal Care and Use Committee of Biopolis (Singapore). All experiments involving rats were carried out following the guidelines and protocols approved by the Institutional Animal Care and Use Committee of Central Michigan University.

Three male Sprague-Dawley rats (RRID:RGD_5508397) from an in-house colony were lesioned with 6-OHDA at 8–9 weeks of age (300–350 g body weight). Several months later, rats underwent surgery for virus injection and cannula placement and were tested for rotational behavior one month later. Rats were housed individually, with free access to food and water.

Stereotactic surgery

6-OHDA lesioning—Rats were under isofluorane anesthesia. The scalp was incised and retracted, and the skull cleaned and dried. Using a stereotaxic frame (Kopf Instruments, Tujunga, CA), rats received 6-OHDA injections into the right medial forebrain bundle (MFB) to produce unilateral lesions of the nigrostriatal pathway. A burr hole was drilled at the MFB coordinates established by Paxinos and Watson: AP −4.4, lateral 1.2, DV −7.8, measured from bregma. 6-OHDA hydrobromide (Sigma-Aldrich) was dissolved in 0.9% saline, containing 0.1% ascorbic acid, at a concentration of 3 mg/ml. Using a 10 μl Hamilton syringe 6-OHDA was injected at a rate of 0.33 μl/min for a total of 4 μl, or 12 μg of 6-OHDA. The needle was kept in place for 2 min following injection, and removed over an additional period of 2 min.

Virus injection—Burr holes were drilled on the right side at coordinates (from Bregma) AP +1, lateral +2.7, and AAV-LMO4 was injected into the right striatum by lowering a 35G beveled injection needle attached to a 10-μl NanoFil syringe (World Precision Instruments, Sarasota, FL) to −5 DV. A first injection of 0.8 μl was made over 8 min, using an automatic microinjector (Stoelting, 780310S); the needle was left in place for an additional 4 min. This was repeated twice, at −4.5 DV and at −4 DV.

Cannula placement—Virus injection was followed by cannula placement. Burr holes were drilled on the left side at coordinates (from Bregma) AP −0.9, lateral −1.4. A 22G guide cannula (3.5 mm length; model C313GS, Plastics One, Roanoke, VA) was gently inserted through the left burr hole to penetrate the brain to the depth of the lateral ventricle. The guide cannula was held in place with dental acrylic bonded to a stainless steel screw anchored to the skull. A dummy cannula (C313DCS, 3.6 mm length) was inserted into each guide cannula and remained in place except during injections.

Lateral Ventricle Injections

Water-soluble native CTZ was prepared at a concentration of 1.6 mM. Rats received an intraventricular injection of 50 μl of CTZ solution or vehicle solution (buffer only without CTZ) before amphetamine injection and testing for rotational behavior. Assuming around 350 μl of cerebrospinal fluid (CSF), the final concentration of CTZ in the CSF is expected to be around 200 μM. The injections were performed at a rate of 0.5 μl per min using an

automatic injector, a Hamilton syringe, and an internal cannula injector (Plastics One) that extended 1 mm beyond the tip of the guide cannula.

Rotational Behavior

Amphetamine rotation was utilized to assess the percentage of dopaminergic fiber loss within the striatum after 6-OHDA surgery, and the level of recovery following viral injection and CTZ or vehicle application. For each test, the animal was given an intraperitoneal injection of 2.5 mg/kg of amphetamine and immediately placed into a 25 cm diameter flat bottom bucket. Movements were recorded with a video camera for 60 min. The number of rotations within 5 min bins were counted.

Histological analysis of rat brains

Rats used in the experiments were perfused transcardially with PBS, followed by 4% paraformaldehyde fixative. Brains were postfixed overnight, then cryoprotected in 30% sucrose solution. Brains were frozen in 2-methylbutane and stored at −80°C until sectioning. Brains were sectioned at 30 μm on a cryostat and imaged under a fluorescent microscope (Zeiss Observer; Hamamatsu Orca Flash 4.0 Digital CMOS camera).

Statistical Analysis

Data are presented as mean ± SEM. All statistical tests were performed in SPSS (IBM). Comparisons between two groups were performed with the unpaired Student's t-test (two-tailed). $P < 0.05$ was considered statistically significant.

RESULTS

GLucM23 emits more light than wild type *Gaussia* luciferase

GLucM23 was generated through random mutagenesis by error-prone PCR (Lindberg et al., 2013) and contains five amino acid changes compared to wild type GLuc: K25E, M35L, V88D, M102I, G159D (Fig. 1A). We fused GLucM23 to *Volvox* channelrhodopsin 1 (VChR1; Ernst et al., 2008; Zhang et al., 2008) to generate LMO4 (GLucM23-VChR1-EYFP) and to the anion channelrhodopsin, iChloC (Wietek et al., 2015), to create the inhibitory iLMO4 (GLucM23-iChloC-EYFP).

GLucM23 reportedly has roughly 10 times higher luminescence output than the wild type luciferase (Lindberg et al., 2013). Because this comparison was carried out with the luciferase either bound to the outer cell membrane or localized to the endoplasmic reticulum, we first examined the light emission of GLucM23 under conditions appropriate for use in luminopsins. We therefore measured light emission from GLucM23 when fused to VChR1, to permit direct comparison to previous LMO versions with luciferase–VChR1 fusions. The different GLuc variants were fused to VChR1 using the same 15 amino acid linker (Berglund et al., 2013); levels of expression of the different constructs were comparable, as determined by measuring fluorescent emission from the attached EYFP reporter. When treated with the luciferase substrate, coelenterazine (CTZ), the GLucM23 moiety in LMO4 was significantly brighter than either wild type or superluminescent GLuc,

and was comparable in bioluminescence activity to the sbGLuc moiety in LMO3 (Figs. 1B and C).

Higher coupling efficiency of GLucM23 improves functional properties of LMO4 and iLMO4

To evaluate the performance of LMO4 and iLMO4, whole-cell patch clamp recordings were made from cultured hippocampal neurons expressing these constructs. We began by measuring, under voltage clamp conditions, the photocurrents evoked by exciting the opsin actuators directly via illumination by an arc lamp (470 nm). For cells expressing LMO4, illumination evoked an inward photocurrent due to activation of VChR1 (Fig. 2A). This current reached a peak within a few ms and exhibited a sustained plateau that persisted for as long as the excitation light was maintained (1 s in the example shown in Fig. 2A). The photocurrents evoked by such direct activation of LMO4 were quite large; when measured at a holding potential of −60 mV, peak photocurrent amplitude ranged from 350 pA to 2 nA (Fig. 2B) and had a mean amplitude of 954 ± 340 pA (n = 18).

In contrast, illumination of neurons expressing iLMO4 generated outward photocurrents (Fig. 2C). These currents also reached a peak rapidly but decreased with sustained activation (4 s for the example shown in Fig. 2C). The reversal potential for this current was approximately −60 mV, consistent with the Cl^- equilibrium potential of −64 mV in our experimental conditions. Photocurrents evoked in neurons expressing iLMO4 were smaller than those evoked in neurons expressing LMO4 (Fig. 2D); at holding potential of −40 mV, mean peak amplitude of these photocurrents was 97 ± 13 pA (n = 13).

To determine the effectiveness of these new LMOs for chemogenetic control of neuronal activity, we measured the ability of CTZ to induce currents in cultured hippocampal neurons expressing LMO4 or iLMO4. In these experiments, bioluminescence emission from the GLucM23 moiety was monitored simultaneously to define the timing of LMO activation during CTZ treatment (Berglund et al., 2013; 2016). Local application of CTZ onto LMO4-expressing neurons yielded bioluminescence emission and simultaneous activation of an inward current (Fig. 3A). This inward current generally tracked the time course of the CTZ-induced light signal and has a mean peak amplitude of 336 ± 77 pA (n = 18). Similarly, treatment of iLMO4-expressing neurons with CTZ induced an outward current (Fig. 3B). This current also tracked the timing of the CTZ-induced bioluminescence signal and had a mean amplitude (at −40 mV) of 39 ± 6 pA (n = 13).

One of the most important determinants of LMO function is the efficiency of coupling between the luciferase light source and the opsin actuator, with 10-fold improvement in coupling efficiency from LMO1 to LMO2, and again from LMO2 to LMO3, leading to the first probe that allows non-invasive manipulation of animal behavior (Berglund et al., 2013; 2016). To determine the coupling efficiencies of LMO4 and iLMO4, we employed the procedure introduced by Berglund et al. (2013). In brief, this procedure compares the magnitude of currents induced by CTZ to those evoked by maximal exposure to light from an arc lamp, with the slope of plots correlating these two responses yielding the coupling coefficient. This procedure takes into account cell-to-cell variations in LMO expression and the coupling coefficient defines the intrinsic efficiency of coupling between luciferase and opsin.

In general, there was a good correlation between the magnitude of CTZ-induced currents and lamp-induced currents for both LMO4 (Fig. 4A) and iLMO4 (Fig. 4B). For each LMO, there was a roughly linear relationship between the two responses (r^2 = 0.93 for LMO4 and 0.95 for iLMO4). Linear regression analysis of the slopes of these functions yielded estimates of the coupling efficiency. For LMO4, the coupling efficiency was 26 ± 7%. This value is remarkably high, approximately 2.6-fold higher than LMO3, the most efficient LMO previously described (Berglund et al., 2016). The coupling efficiency for iLMO4 was even higher, being 36 ± 6%. As can be seen by comparing the properties of these LMO4 versions to previous generations of LMOs (Table I), LMO4 and iLMO4 each represent substantial improvements in performance compared to previous LMOs.

Chemogenetic and optogenetic control of neuronal activity by LMO4 and iLMO4

To examine the ability of LMO4 and iLMO4 to control neuronal activity, we examined their effects on the membrane potential of cultured hippocampal neurons expressing these LMOs. Exposure to arc lamp light depolarized the membrane potential and evoked action potentials in neurons expressing LMO4. Conversely, such illumination hyperpolarized iLMO4-expressing neurons and inhibited their ability to fire action potentials in response to depolarizing current steps. Thus, the VChR1 and iChloC opsin moieties retain their ability to control membrane potential, as expected from their ability to generate photocurrents (Fig. 2).

To determine the ability of the new LMOs to control neuronal activity via chemogenetics, we next examined the effects of CTZ treatment. For the case of neurons expressing LMO4, CTZ treatment produced a transient depolarization of the membrane potential (Fig. 5A). The mean amplitude of these CTZ-induced membrane potential changes was 12.6 ± 6.6 mV (n = 8). For these cultured hippocampal neurons, this amount of depolarization was insufficient to induce action potential firing. However, this CTZ response would be expected to induce a strong depolarizing bias on responses of these neurons to excitatory synaptic inputs and would be sufficient to induce action potential firing in neurons with higher input resistance and/or with resting potentials closer to action potential threshold.

Treatment of iLMO4-expressing neurons with CTZ application induced a large increase in the frequency of spontaneous excitatory postsynaptic potentials (EPSPs), resulting in a paradoxical excitation of neurons expressing this inhibitory LMO (Figs. 5D and E). Pre-treatment of cultures with kynurenic acid (2 mM), a glutamate receptor antagonist (Bekkers and Stevens, 1991), blocked the CTZ-induced increase in EPSP frequency (Fig. 5F). Under these conditions, CTZ treatment inhibited the ability of the iLMO4-expressing neurons to fire action potentials in response to brief depolarizing current pulses (Fig. 5G). This suggests that the increase in EPSP frequency observed in the absence of kynurenic acid was due to disinhibition of presynaptic excitatory neurons that received inhibitory synaptic input from interneurons. The same results were observed in response to arc lamp illumination (Fig. 5B and C). Thus, iLMO4 expression is sufficient to produce CTZ-induced suppression of action potential firing in cultured hippocampal neurons.

We also used multi-electrode extracellular recordings to examine the ability of iLMO4 to silence neuronal populations (Figs. 6 and 7). For these experiments, we transduced the entire population of rat embryonic cortical neurons in an MEA well with AAV-hSyn-iLMO4, using

a virus titer that yielded transduction of most neurons by iLMO4 (Fig. 6A). The effects of CTZ were compared to that of an arc lamp. Photostimulation of iLMO4 resulted in complete silencing of spontaneous spiking activity that started and ended precisely with the application of light (see Fig. 6B for individual recording example, and Fig. 7B for mean spiking activity across several electrodes; t20, 14.210, P = 3.2495E-12, n = 21). In contrast, spiking frequency was increased in spontaneously spiking neuronal cultures expressing the activating LMO4 (Fig. 7A; t32, 8.836, P = 2.195E-10, n = 33). Addition of CTZ to MEA cultures expressing iLMO4 for a final concentration of 0.5 μM did not significantly alter spontaneous spiking frequency (see Fig. 6C for individual recording example, and Fig. 7C for mean spiking activity; t14, 0.240, P = 0.406851772, n = 15). However, when CTZ was added for a final concentration of 50 μM, robust silencing of activity was observed (see Fig. 6D for individual recording example, and Fig. 7D for mean spiking activity; t11, 3.957, P = 0.001123, n = 12). Silencing was complete for 7 min in the example shown (Fig. 6E), and on average for 10 min (data not shown), at which time spontaneous spiking activity started up again to resume pre-CTZ frequencies within 30 min. These results indicate that the optogenetic element in iLMO4 can be activated by both physical and biological light sources and that CTZ can provide sufficient inhibitory drive to silence spontaneous activity in a population of neurons.

LMO4 attenuates rotational behavior in 6-OHDA-lesioned rats *in vivo*

We utilized an established paradigm for testing the efficacy of LMO4 to affect behavior. Unilateral destruction of dopaminergic fibers to the striatum by chemical lesioning of the medial forebrain bundle induces ipsiversive circling behavior in rats after amphetamine stimulation (Hefti et al., 1980). Ipsiversive rotations can be reduced by reconstituting dopaminergic drive directly from the striatum, for example by transplantation of dopaminergic neurons (Dunnett et al., 1981). We assessed whether viral mediated LMO4 expression in the right striatum would attenuate amphetamine induced right rotations with CTZ application to the ventricular system. We used only male animals for these studies, as our focus was on comparing the change in rotations within individual animals after application of CTZ versus vehicle. Thus, no inferences can be made as to any gender specific effects. Rats with medial forebrain bundle lesions on the right side were pre-tested for robust ipsilateral rotations after amphetamine injection. Animals received injections of AAV expressing LMO4 under control of the human synapsin promoter into the right striatum. A permanent cannula was placed into the left lateral ventricle. Several weeks after the surgeries rats received, via the cannula, CTZ or vehicle; this was reversed (vehicle or CTZ) for each animal after another several weeks. Application of CTZ or vehicle was immediately followed by amphetamine injection and recording of movements. During a one-hour recording session, vehicle injected rats displayed the same rotational behavior at the beginning (first 15 min) as at the end (last 15 min; Fig. 8A). In contrast, ipsiversive rotations in CTZ injected animals were significantly decreased in the initial 15 min after CTZ application; rotations returned to the expected number of turns typical for a given animal by the last 15 min (Fig. 8A; t2 = 12.509, P = 0.003165, n = 3 per group). Robust expression of LMO4 in the striatum was confirmed by EYFP expression in serial sections (Fig. 8B).

DISCUSSION

This study reveals that GLucM23, a recently described variant of *Gaussia* luciferase, is an efficient light source for activating optogenetic elements in bioluminescence-driven optogenetics. The fusion of GLucM23 with *Volvox* channelrhodopsin-1 and the anion channelrhodopsin iChloC, a depolarizing and hyperpolarizing channelrhodopsin, respectively, produced LMO4 and iLMO4. Both luminopsins proved very efficient in activating and silencing neurons, respectively, via CTZ mediated light emission of GLucM23. Bioluminescence-driven optogenetic activation and silencing was demonstrated in single cell recordings, multi-electrode recordings, and by affecting behavior.

Higher coupling efficiencies between the light-emitting luciferase and the light-sensing opsin can be achieved, in principle, by increasing either or both the light emission of the luciferase and the light-sensitivity of the opsin. We previously improved performance of luminopsins by switching out ChR2 in LMO1 with VChR1 in LMO2, then improved from subthreshold depolarization to eliciting action potentials by switching from wild type GLuc in LMO2 (Berglund et al., 2013) to slow burn GLuc in LMO3 (Berglund et al., 2016). The improvement in each round was about 10-fold (see also Table I). The coupling efficiency of both new LMOs was higher than of LMO3 by a factor of 2–3. Nevertheless, the new version of GLuc, GLucM23, in combination with VChR1 in LMO4, is at least as robust as LMO3. Combining GLucM23 with the light-sensitive chloride channel iChloC in iLMO4 generates a probe which is highly efficient in silencing neuronal activity. These new LMOs, LMO4 and iLMO4, will be useful in bimodal opto- and chemogenetic experiments of neural control.

Acknowledgments

This work was supported by the National Institutes of Health (R21MH101525; R21EY026427; U01NS099709), the National Science Foundation (CBET-1464686), the W.M. Keck Foundation, grant 2015-T1-001-069 from the Singapore Ministry of Education, and the World Class Institute (WCI) program of the National Research Foundation of Korea (NRF) funded by the Ministry of Science, ICT & Future Planning (WCI 2009-003).

References

Bekkers JM, Stevens CF. Excitatory and inhibitory autaptic currents in isolated hippocampal neurons maintained in cell culture. Proc Natl Acad Sci U S. 1991; 88:7834–8.

Berglund K, Birkner E, Augustine GJ, Hochgeschwender U. Light-Emitting Channelrhodopsins for Combined Optogenetic and Chemical-Genetic Control of Neurons. PLoS One. 2013; 8:e59759. [PubMed: 23544095]

Berglund K, Clissold K, Li HE, Wen L, Park SY, Gleixner J, Klein ME, Lu D, Barter JW, Rossi MA, Augustine GJ, Yin HH, Hochgeschwender U. Luminopsins integrate opto- and chemogenetics by using physical and biological light sources for opsin activation. Proc Natl Acad Sci U S A. 2016; 113:E358–67. [PubMed: 26733686]

Dragulescu-Andrasi A, Chan CT, De A, Massoud TF, Gambhir SS. Bioluminescence resonance energy transfer (BRET) imaging of protein – protein interactions within deep tissues of living subjects. Proc Natl Acad Sci U S A. 2011; 108:12060–5. [PubMed: 21730157]

Dunnett SB, Björklund A, Stenevi U, Iversen SD. Behavioral recovery following transplantation of substantia nigra in rats subjected to 6-OHDA lesions of the nigrostriatal pathway. II. Bilateral lesions. Brain Res. 1981; 229:457–70. [PubMed: 6796197]

Fenno L, Yizhar O, Deisseroth K. The development and application of optogenetics. Annu Rev Neurosci. 2011; 34:389–412. [PubMed: 21692661]

Gradinaru V, Thompson KR, Deisseroth K. eNpHR: a Natronomonas halorhodopsin enhanced for optogenetic applications. Brain Cell Biol. 2008; 36:129–39. [PubMed: 18677566]

Guo P, El-Gohary Y, Prasadan K, Shiota C, Xiao X, Wiersch J, Paredes J, Tulachan S, Gittes GK. Rapid and simplified purification of recombinant adeno-associated virus. J Virol Methods. 2012; 183:139–46. [PubMed: 22561982]

Hefti F, Melamed E, Sahakian BJ, Wurtman RJ. Circling behavior in rats with partial, unilateral nigro-striatal lesions: effect of amphetamine, apomorphine, and DOPA. Pharmacol Biochem Behav. 1980; 12:185–188. [PubMed: 7189592]

Kim SB, Suzuki H, Sato M, Tao H. Superluminescent variants of marine luciferases for bioassays. Anal Chem. 2011; 83:8732–40. [PubMed: 21951281]

Lindberg E, Mizukami S, Ibata K, Miyawaki A, Kikuchi K. Development of Luminescent Coelenterazine Derivatives Activatable by β-Galactosidase for Monitoring Dual Gene Expression. Chemistry. 2013; 19:14970–14976. [PubMed: 24105816]

Nagel G, Szellas T, Huhn W, Kateriya S, Adeishvili N, Berthold P, Ollig D, Hegemann P, Bamberg E. Channelrhodopsin-2, a directly light-gated cation-selective membrane channel. Proc Natl Acad Sci U S A. 2003; 100:13940–5. [PubMed: 14615590]

Saito K, Chang YF, Horikawa K, Hatsugai N, Higuchi Y, Hashida M, Yoshida Y, Matsuda T, Arai Y, Nagai T. Luminescent proteins for high-speed single-cell and whole-body imaging. Nat Commun. 2012; 3:1262. [PubMed: 23232392]

Sternson SM, Roth BL. Chemogenetic Tools to Interrogate Brain Functions. Annu Rev Neurosci. 2014; 37:387–407. [PubMed: 25002280]

Tung JK, Gutekunst C-A, Gross RE. Inhibitory luminopsins: genetically-encoded bioluminescent opsins for versatile, scalable, and hardware-independent optogenetic inhibition. Sci Rep. 2015; 5:14366. [PubMed: 26399324]

Verhaegen M, Christopoulos TK. Recombinant Gaussia luciferase. Overexpression, purification, and analytical application of a bioluminescent reporter for DNA hybridization. Anal Chem. 2002; 74:4378–85. [PubMed: 12236345]

Welsh JP, Patel KG, Manthiram K, Swartz JR. Multiply mutated Gaussia luciferases provide prolonged and intense bioluminescence. Biochem Biophys Res Commun. 2009; 389:563–8. [PubMed: 19825431]

Wietek J, Beltramo R, Scanziani M, Hegemann P, Oertner TG, Simon Wiegert J. An improved chloride-conducting channelrhodopsin for light-induced inhibition of neuronal activity in vivo. Sci Rep. 2015; 5:14807. [PubMed: 26443033]

SIGNIFICANCE

Manipulation of neuronal activity in behaving experimental animals is crucial for elucidating neuronal networks underlying brain function. Both optogenetic and chemogenetic approaches continue to be useful for identifying the contributions of genetically-defined neuron populations to circuit and behavioral outputs. Luminopsins, which are fusions of light-emitting luciferases and light-sensing optogenetic elements, provide both acute optical and chronic chemical control in one molecule. Our newest probes, LMO4 and iLMO4, combine a brighter luciferase with activating and silencing opsins for improved bimodal control of neural activity.

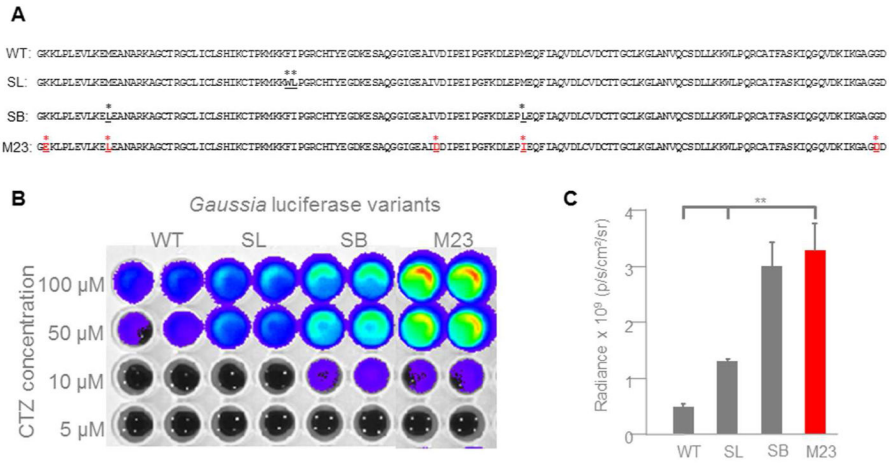

Figure 1.

Gaussia luciferase (GLuc) variants. **A**: Comparison of amino acid sequences of wild type GLuc (WT; position 48 – 185; GenBank number AAG54095.1) to 'superluminescent' (SL; Kim et al., 2011), 'slow burn' (SB; Welsh et al., 2009), and GLucM23 (M23; Lindberg et al., 2013). Amino acid changes are highlighted. **B:** Comparison of bioluminescence emission of GLuc variants. HEK293 cells were lipofected with pcDNA3.1 plasmids of the different GLuc variants fused to VChR1-EYFP. Fluorescence of the EYFP reporter was used to normalize luminance from the GLuc variants. CTZ was added to a final concentration as indicated. Luminance was measured in an IVIS system. The intensity of light emission is represented by pseudo-colors, with red areas representing the highest amount of light emission, and blue/violet areas representing the least. **C:** Comparison of radiance of GLuc variants at 50 µM concentration of CTZ. IVIS measurements of 4 individual samples for each variant were graphed. GLucM23 emits significantly more photons than either wild type GLuc ($P = 0.002235$) or superluminescent GLuc ($P = 0.007356$).

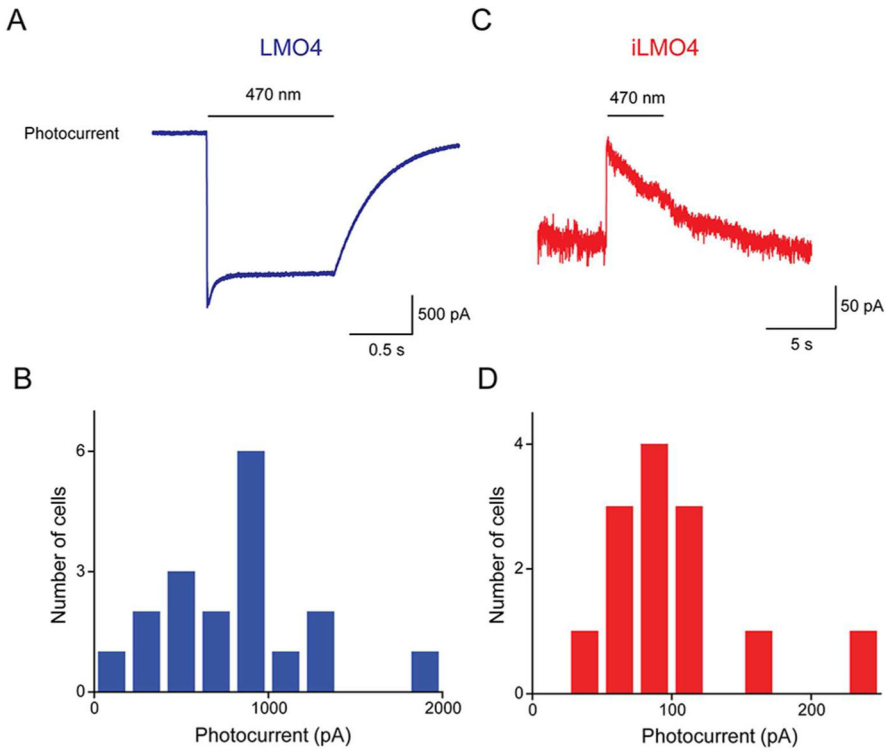

Figure 2.

Photocurrents generated in cultured mouse hippocampal neurons expressing LMO4 or iLMO4. **A:** Photocurrent evoked by arc lamp illumination (470 nm, at bar) in neuron expressing LMO4. **B:** Distribution of peak photocurrent amplitudes measured in individual LMO4-expressing neurons. **C:** Photocurrent evoked by arc lamp illumination (470 nm, at bar) in neuron expressing iLMO4. **B:** Distribution of peak photocurrent amplitudes measured in individual iLMO4-expressing neurons.

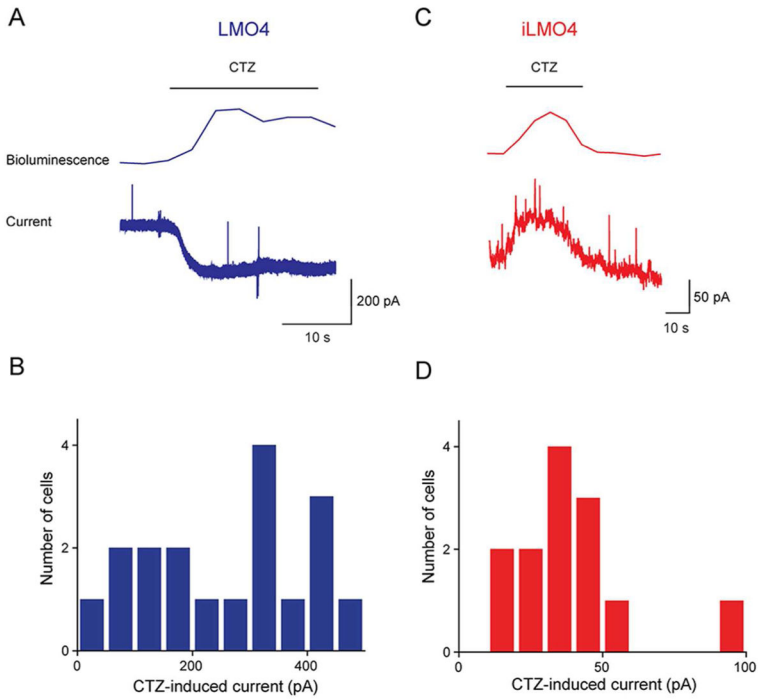

Figure 3.

CTZ-induced currents generated in cultured mouse hippocampal neurons expressing LMO4 or iLMO4. **A:** Representative bioluminescence emission and inward current evoked by CTZ application (at bar) in neuron expressing LMO4. **B:** Distribution of peak amplitudes of CTZ-induced currents measured in individual LMO4-expressing neurons. **C:** Representative bioluminescence emission and inward current evoked by CTZ application (at bar) in neuron expressing iLMO4. **D:** Distribution of peak amplitudes of CTZ-induced currents measured in individual iLMO4-expressing neurons.

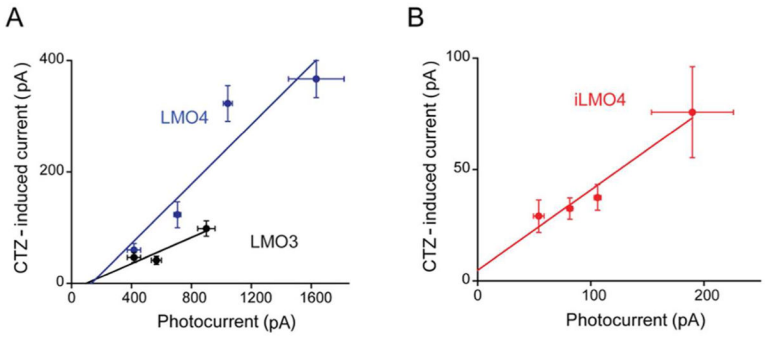

Figure 4.

Improved coupling efficiency of LMO4 and iLMO4. **A:** Correlation between photocurrents induced by arc lamp illumination and CTZ-induced currents for neurons expressing either LMO3 (black) or LMO4 (blue). Slope of linear regression fit to data indicates the coupling coefficient, which was 0.11 for LMO3 (n = 9) and 0.26 for LMO4 (n = 18). **B:** Correlation between photocurrents induced by arc lamp illumination and CTZ-induced currents for neurons expressing iLMO4. Slope of relationship, the coupling coefficient, is 0.36 (n = 13).

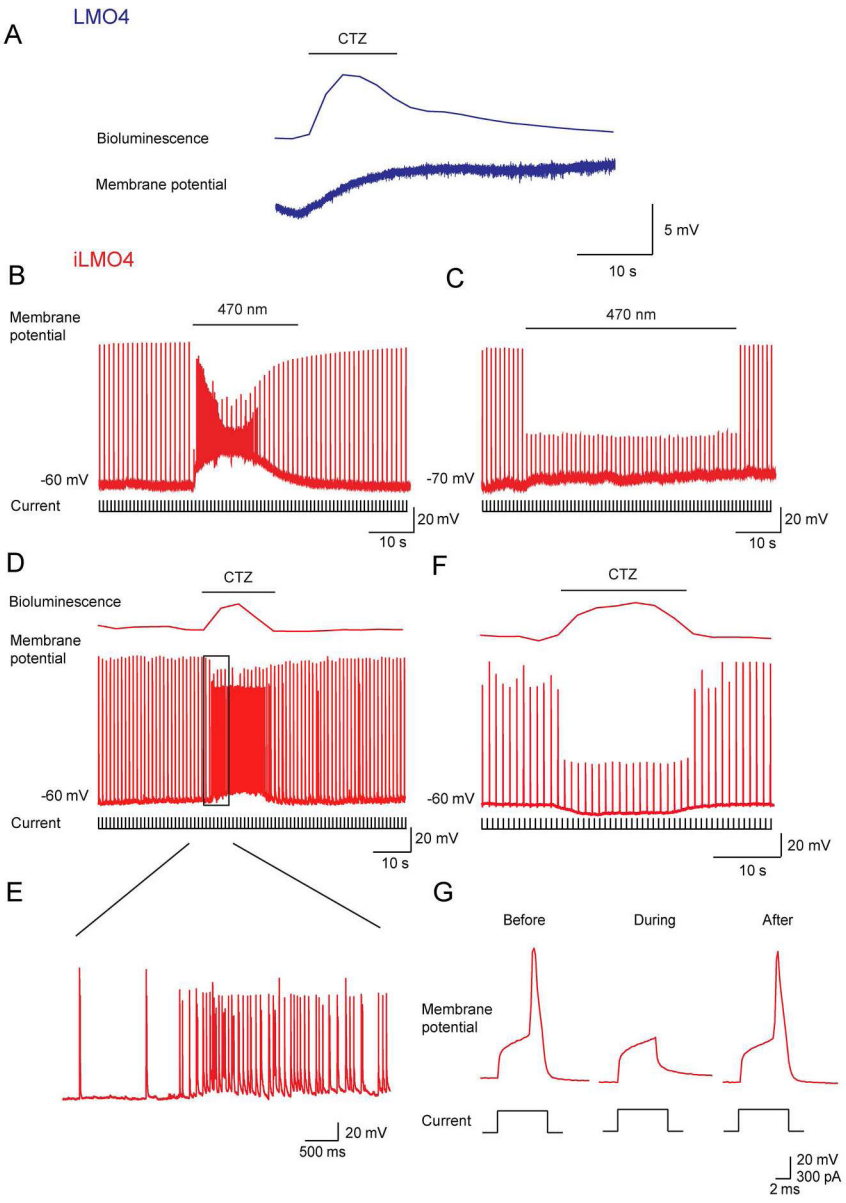

Figure 5.

CTZ-induced membrane potential changes in cultured mouse hippocampal neurons expressing LMO4 or iLMO4. **A**: CTZ-induced membrane potential change in neuron expressing LMO4. **B**: Application of depolarizing current pulses (lower) evoked action potentials (middle) in a neuron expressing iLMO4. Arc lamp illumination (470 nm; at bar) increased the frequency of spontaneous EPSCs. **C**: Pre-treatment of cultures with the glutamate receptor antagonist, kynurenic acid (2 mM), blocked the light-induced increase in EPSC frequency and revealed a suppression of action potential firing (middle) in response to depolarizing current pulses (lower) during arc lamp illumination (at bar).**D**: The same results were obtained with CTZ. CTZ application (at bar) generated bioluminescence (upper) and increased neuronal activity. **E:** Examination of CTZ response (black rectangle in D) with higher time resolution indicates an increase in the frequency of spontaneous EPSPs. **F:** After

treatment with kynurenic acid (2 mM), CTZ application (at bar) yielded bioluminescence (upper) and a suppression of action potential firing (middle) in response to depolarizing current pulses (lower). **G:** Membrane potential responses to depolarizing current responses were attenuated during CTZ treatment, in this case abolishing action potential firing.

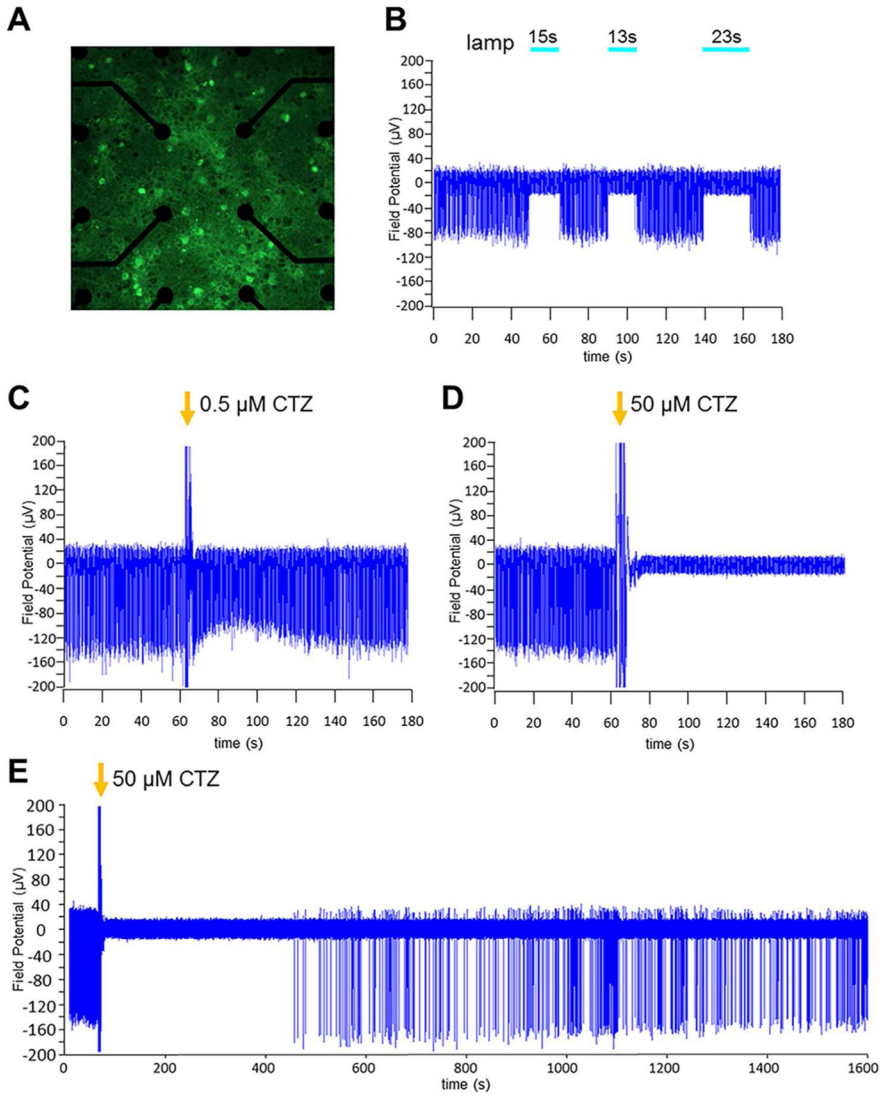

Figure 6.

Multi-electrode recordings from cortical neurons transduced with AAV-hSyn- iLMO4. Primary embryonic rat cortical neurons were plated in one-well MEAs and transduced with virus. Two weeks later activity of spontaneously spiking neurons was recorded. **A**: Fluorescent image of iLMO4 expressing neurons (green) on the center electrodes (black circles) of the MEA, 40 x objective. **B–D:** Recordings from iLMO4-transduced neurons from one channel under different conditions. **B:** Application of blue light from an arc lamp for 10 and 20 s. Neurons are silenced for the time they are exposed to light. **C:** Addition of CTZ (arrow) to the MEA well for a final concentration of 0.5 μM. Large amplitude spikes coinciding with addition of CTZ are artifacts from disturbing the culture. Spiking frequency does not change with addition of CTZ at this low concentration. **D:** Addition of CTZ (arrow) to the MEA well for a final concentration of 50 μM. CTZ application is followed by complete silencing of neuronal spiking. **E:** Extended display of recording with 50 μM CTZ (D). Neuronal activity resumes around 7 min after CTZ induced silencing.

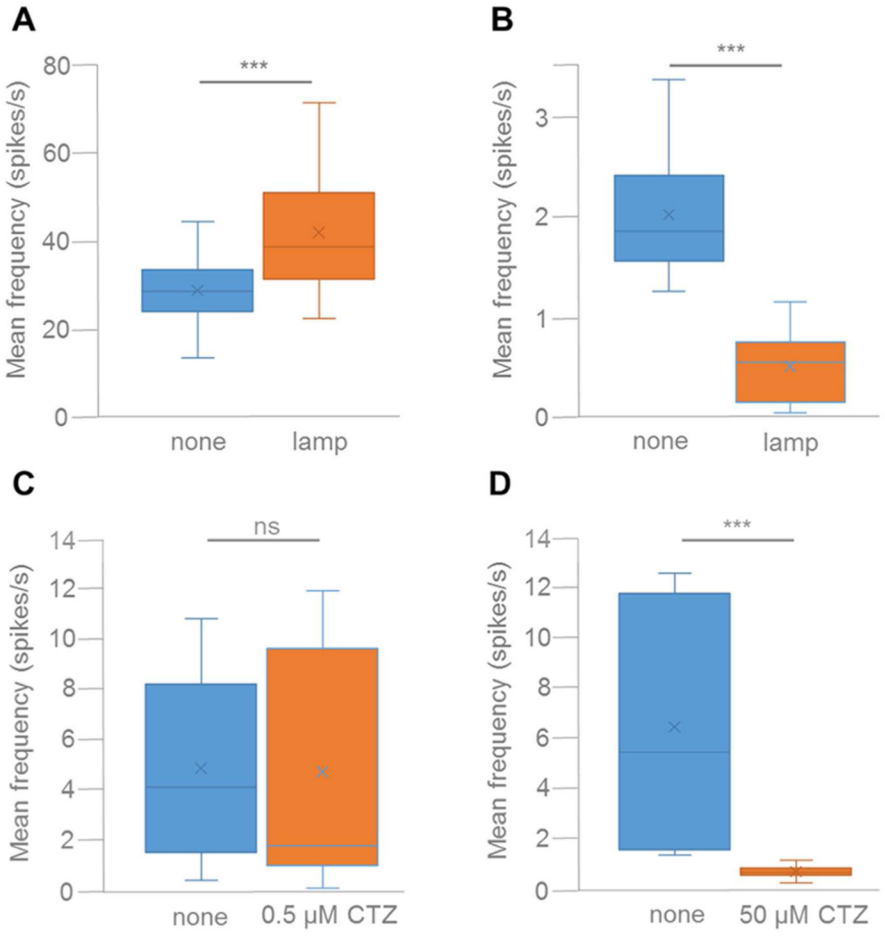

Figure 7.

Average spiking frequencies of five MEA channels before any treatment (blue bars) and after application of physical (A, B) or biological (C, D) light (orange bars). **A:** Neurons were transduced with AAV-hSyn-LMO4. Spiking frequency increased significantly when neurons were exposed to light from an arc lamp ($P < 0.0001$). **B–D:** Neurons were transduced with AAV-hSyn-iLMO4. Spiking frequency decreased significantly when neurons were exposed to light from an arc lamp (**B**; $P < 0.0001$) and with application of 50 μM CTZ (**D**; $P < 0.001$), but did not change significantly with application of 0.5 μM CTZ (**C**).

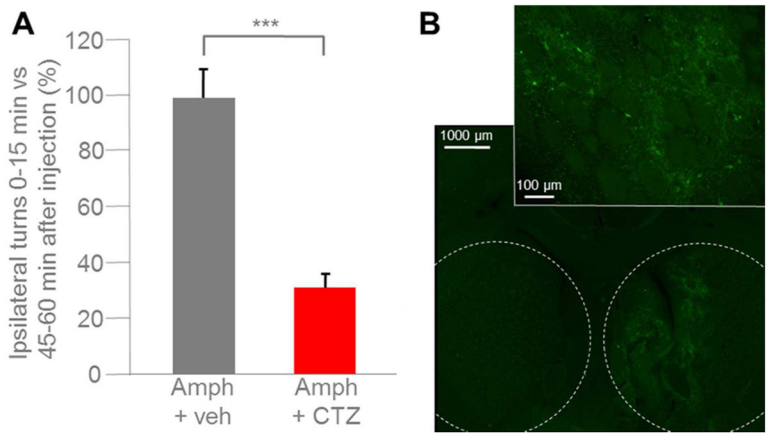

Figure 8.

Amphetamine-induced rotational behavior attenuated by LMO4. Adult male rats (n = 3) were injected with 6-OHDA into the right hemisphere with coordinates set to target the medial forebrain bundle. AAV-hSyn-LMO4 was injected into the right striatum. A lateral ventricle cannula was implanted into the left hemisphere. For testing rotational behavior rats were injected intraperitoneally with amphetamine (2.5 mg/kg), and ipsilateral rotations were counted for the first and last 15 min of an hour. **A:** The same three animals were tested with vehicle injection (Amph + veh) and with CTZ injection at the time of amphetamine application (Amph + CTZ; final concentration of 200 µM in CSF). Bars indicate mean percent of amphetamine-induced ipsilateral rotations during the first 15 min of testing. Data are normalized relative to number of turns during the last 15 min (between 45 to 60 min after amphetamine injection). CTZ, but not vehicle, decreases the number of ipsilateral rotations significantly for the first 15 min after injection ($P = 0.002017$). **B:** Fluorescence images of a coronal section from a rat at the end of the experiment. Stippled lines in overview image (5x) mark right and left striatum; higher magnification image (20x) zooms in on right striatum. Neurons expressing LMO4 show green fluorescence from the EYFP reporter.

TABLE I

Efficiency of Coupling Between Different Luciferase Variants and Opsins

Luminopsin			Luciferase	Opsin	Coupling Efficiency (%)	Reference
Excitatory LMOs	LMO1	GLuc-ChR2	Gaussia (wildtype)	ChR2	0.1	Berglund et al. 2013
	LMO2	GLuc-VChR1	Gaussia (wildtype)	VChR1	1.2	Berglund et al. 2013, 2016
	LMO3	sbGLuc-VChR1	Gaussia (slow burn)	VChR1	11	Berglund et al. 2016
	LMO4	GLucM23-VChR1	Gaussia (M23 mutant)	VChR1	26	this paper
Inhibitory LMOs	iLMO1	NpHR-TagRFP-RLuc	Renilla (TagRFP)	NpHR	nd	Tung et al. 2015
	iLMO2	NpHR-NanoLantern	Renilla (NanoLantern)	NpHR	21	Tung et al. 2015
	iLMO	slGLuc-Mac	Gaussia (superluminescent)	Mac	nd	Berglund et al. 2016
	iLMO4	GLucM23-iChloC	Gaussia (M23 mutant)	iChloC	36	this paper

nd, not determined